

Nuclear spectroscopy of the heaviest elements: studies of ^{254}No , ^{257}Rf , and ^{261}Sg

J S Berryman¹, R M Clark¹, K E Gregorich¹, J M Allmond², D L Bleuel³, R J Cooper⁴, M Cromaz¹, M A Deleplanque¹, I Dragojević^{1,5}, J Dvorak¹, P A Ellison^{1,5}, P Fallon¹, M A Garcia^{1,5}, J M Gates¹, S Gros¹, O Gothe^{1,5}, H B Jeppesen¹, D Kaji⁶, I Y Lee¹, A O Macchiavelli¹, K Morimoto⁶, H Nitsche^{1,5}, S Paschalis¹, M Petri¹, J Qian¹, L Stavsetra^{1,5}, F S Stephens¹, M A Stoyer³, T J Ross², H Watanabe⁶ and M Wiedeking³

¹ Lawrence Berkeley National Laboratory, Berkeley, California 94720, USA

² Department of Physics, University of Richmond, Virginia 23173, USA

³ Lawrence Livermore National Laboratory, Livermore, California 94551, USA

⁴ Physics Division, Oak Ridge National Laboratory, Oak Ridge, Tennessee 37831, USA

⁵ Department of Chemistry, University of California, Berkeley, California 94720, USA

⁶ Nishina Centre for Accelerator Based Science, RIKEN, Wako, Saitama 351-0198, Japan

E-mail: berrymaj@nscl.msu.edu

Abstract. Recently it has become possible to perform detailed spectroscopy on nuclei beyond $Z = 100$ with the aim of understanding the underlying single-particle structure of superheavy elements. A number of such experiments have been performed at the 88-Inch Cyclotron of the Lawrence Berkeley National Laboratory using the Berkeley Gas-filled Separator (BGS), coupled with delayed γ -ray and electron-decay spectroscopy. Experiments have been performed on ^{254}No ($Z = 102$), ^{257}Rf ($Z = 104$), and ^{261}Sg ($Z = 106$). The results provide new information on the properties of transactinide nuclei, which is important for testing models of the heaviest elements.

1. Introduction

Superheavy nuclei should fission instantaneously due to the Coulomb repulsion between protons. However, nuclear shell effects provide added stability due to energy gaps in the single-particle level ordering at particular “magic” numbers of protons and neutrons. The spherical shell closures beyond ^{208}Pb remain a matter of considerable theoretical debate. The microscopic-macroscopic models with various parameterizations of the nuclear potential predict magic numbers at $Z = 114$ and $N = 184$ [1]. Meanwhile, relativistic and nonrelativistic nuclear mean-field calculations yield a proton magic number ranging from $Z = 120$ to 126 and a neutron magic number ranging from $N = 172$ to 184 [2, 3]. The heaviest element whose existence has been confirmed has $Z = 114$ [4, 5], with further experiments suggesting the observation of elements up to $Z = 118$ [6]. The production cross sections for the superheavy elements drop rapidly with proton number and are on the order of a few pb for element 114 [4, 5, 7]. Recently, it has become possible to take a new approach to understanding the behavior of the heaviest nuclei by

making detailed spectroscopic studies of shell-stabilized nuclei in the vicinity of deformed sub-shell gaps at $Z \approx 100$ and $N \approx 152$ (^{252}Fm) [8]. Some nuclei in this region have production cross sections up to a few μb and therefore are far easier to access experimentally. Prolate deformation drives down single-particle orbitals from above the predicted $Z = 114$ and $N = 184$ gaps, which can intrude close to the Fermi surface in the trans-fermium region. Such experimental data is essential for testing the models that differ in their predictions for the superheavy elements.

The particular interest of these studies is the decay of isomers, excited metastable states of atomic nuclei. Isomers with high angular momentum are found in deformed nuclei near ^{252}Fm ($Z = 100$, $N = 152$). Isomers in this region, both single and multi-quasiparticle (qp) states, may involve nucleon orbitals with high K values, where K is the quantum number describing the projection of the total angular momentum on the symmetry axis. Electromagnetic decays from these states can involve large changes of K and such transitions can become hindered, leading to the metastability. One can learn about single-particle structure, pairing correlations, and excitation modes in the heaviest nuclei by identifying such isomers and studying their decay to states with lower excitation energy.

2. Experimental Details

All experiments were performed at the 88-Inch Cyclotron of the Lawrence Berkeley National Laboratory using the Berkeley Gas-filled Separator (BGS) [9]. The experimental conditions are given in Table 1. The beam from the cyclotron passed through a $\approx 45 \mu\text{g}/\text{cm}^2$ carbon window (separating the 0.5-Torr He gas inside the BGS from the beamline vacuum) and was incident on the targets. The targets comprised a stack of two Pb foils; each foil had a thickness of $\approx 0.4 \text{ mg}/\text{cm}^2$ and was evaporated on $\approx 35 \mu\text{g}/\text{cm}^2$ carbon backing. The targets were placed on a rotating target wheel, positioned such that the beam was incident on the target backing first. The average beam intensity was about 300 pnA for all experiments. Evaporation residues were separated from the beam and other reaction products by their differing magnetic rigidities in He before being implanted in a 1-mm thick 16×16 double-sided silicon strip detector (DSSD) with an active area of $5 \times 5 \text{ cm}$. A standard HPGe clover detector [10] was mounted behind the 2 mm Al backplate of the BGS focal plane at approximately 5 mm from the DSSD. Standard γ -ray sources were used for energy and efficiency calibrations. The focal plane distribution of recoils was simulated, yielding an absolute photopeak efficiency of $\approx 17\%$ at 122 keV and $\approx 3.5\%$ at 1 MeV. All of the γ -ray spectra were created by treating the four clover crystals as individual detectors (no addback) in the analysis described below. In all cases, an isomer decay tagging technique was followed as described by Jones *et al.* [11]. Recoils were identified by an MWPC signal in coincidence with an implant in a DSSD pixel. The electromagnetic decay of isomers were identified by searching for one or more delayed electron signals ($50 \text{ keV} < E_{\text{electron}} < 2000 \text{ keV}$), within the same pixel of the DSSD as an implanted recoil (labeled as a recoil-electron, r-e, event or r-e-e in the case of two electrons). In some cases when the α decay of the recoil was short ($< 10 \text{ s}$), recoil- α events (labeled r- α) and recoil-electron- α (labeled r-e- α) events were also identified, all within the same pixel of the DSSD.

Table 1: Experimental conditions.

	^{254}No	^{257}Rf	^{261}Sg
Reaction	$^{208}\text{Pb}(^{48}\text{Ca},2n)$	^{254}No	$^{208}\text{Pb}(^{50}\text{Ti},n)$
Beam Energy (MeV)	221	238	261
Cross section	$2 \mu\text{b}$ [12]	40 nb [13]	1.9 nb [14]

3. Results

3.1. Decay of ^{254}No

The results discussed below on ^{254}No were first reported by our group in the paper by Clark *et al.* [15]. A total of 1.5×10^5 r-e events were recorded, indicating the presence of an isomer. A total of 1.6×10^4 r-e-e events were identified, indicating two isomers. Decay curves from the r-e and r-e-e events yielded half-lives of $184(2)$ μs and $263(2)$ ms, which are in agreement with the previously measured values of the two known isomers in ^{254}No [16, 17]. γ rays were searched in prompt coincidence (± 200 ns) with the isomeric electron signals. The proposed decay scheme is shown in Fig. 1. We agree with the previous studies [16, 17] in regards to the decay of the 263 ms isomer. In addition, we see many more high-energy transitions decaying from each state in the $K^\pi = 3^+$ band to states in the ground-state rotational band. We also clearly observe several of the in-band transitions including the 82 keV in-band $\Delta I = 1$ and 152 keV crossover $\Delta I = 2$ transitions from the 7^+ rotational state. The ratio of their intensities gives a measure of the g factor of the band and we find a value of $|g_K - g_R| = 0.52(6)$ (assuming a quadrupole deformation of $\beta_2 = 0.26$), which is consistent with the previous studies [16, 17]. Further, the agreement in g factors confirms the assignment of $\pi^2([514]7/2^- \otimes [521]1/2^-)$ two quasiproton configuration suggested by the previous studies for the $K^\pi = 3^+$ state.

While the previous decay studies yielded a lower limit for the excitation energy of >2.5 MeV, they were unable to establish a decay scheme for the higher lying isomer. Prominent γ -ray transitions were observed at 133 and 605 keV. As a result of greater statistics, we have been able to establish the decay scheme as presented in Fig. 1. Two possible spin-parity assignments were suggested for the $184 \mu\text{s}$ isomeric state, namely 14^+ [17] and 16^+ [16].

We favor the $K^\pi = 16^+$ assignment since, if the state were 14^+ , we would expect to see additional transitions to lower-lying members of the rotational band for the lower spin assignment and we do not. The lowest in-band state is a new high-K state with $K^\pi = 10^+$. We see two $\Delta I = 2$ crossover transitions associated with the band at 326 and 348 keV. From the ratio of their intensities with their respective $\Delta I = 1$ in-band transitions, we deduce an average g factor of $|g_K - g_R| = 0.38(7)$. From our analysis, the energy of the $K^\pi = 16^+$ state is established as $E_x = 2.928(3)$ MeV, which is consistent with the highest total energy observed for the isomer decay in our experiment (and above the lower limits established in the previous measurements).

There are at least three different possible configurations for the $K^\pi = 8^-$ state including the $\pi^2([514]7/2^- \otimes [624]9/2^+)$ two quasi-proton configuration and either the $\nu^2([734]9/2^- \otimes [624]7/2^+)$ or $\nu^2([734]9/2^- \otimes [613]7/2^+)$ two quasi-neutron configurations, with the latter of these two generally calculated to be the lowest in energy of the quasi-neutron states. All the calculations predict that the lowest-lying proton and neutron two-qp $K^\pi = 8^-$ states have similar excitation energies. Both the previous studies [16, 17], as well as a recent experiment by Heßberger *et al.* [18], favor the quasi-proton assignment since the 8^- isomer is seen to decay to the band based on the $K^\pi = 3^+$ state, which has been unambiguously identified as a two-quasiproton excitation. However, the long half life of the $K^\pi = 8^-$ isomer may be partially due to the transition involving the interchange of both protons and neutrons [16]. We favor a two-

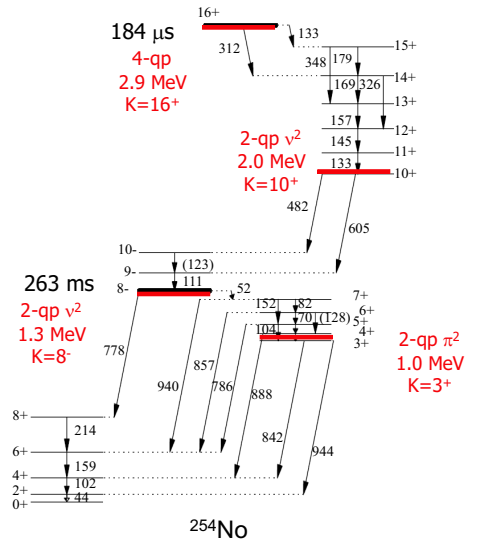


Figure 1: Proposed level scheme for ^{254}No . Transition energies are given in keV. Suggested spins and parities of the states are indicated.

quasineutron configuration for the $K^\pi = 8^-$ isomer. The reason for this is based on the nature of the $K^\pi = 10^+$ state which is decaying directly into the 8^- band. The only possible two-qp configuration that could give rise to such a $K^\pi = 10^+$ excitation is $\nu^2([734]9/2^- \otimes [725]11/2^-)$. The deduced g factor of $|g_K - g_R| = 0.38(7)$ is consistent with this configuration assignment for the 10^+ state. The $K^\pi = 10^+$ state should then favor decay to the in-band states based on a $K^\pi = 8^-$ two quasi-neutron configuration since it involves the transition of a single neutron. The decay to the $K^\pi = 8^-$ two quasi-proton state would involve a transition requiring interchange of both neutrons and protons and would not be favored.

3.2. Decay of ^{257}Rf

The results discussed below on ^{257}Rf were first reported by our group in the paper by Berryman *et al.* [19]. A total of 1904 r- α (^{257}Rf) events were recorded. The half life for all r- α (^{257}Rf) events was deduced to be 4.8 ± 0.2 s, which agrees with the value of 4.7 ± 0.3 s given in a recent paper by Qian *et al.* [20]. There were a total of 1083 r-e events, indicating the presence of an isomer. Conversion electrons coming from the decay of ^{257}Rf were distinguished from those coming from the decay of ^{256}Rf by observing an α decay following the conversion electron in the same pixel of the DSSD. There were 371 such events, labeled r-e- α (^{257}Rf). The time difference between recoil implants and the subsequent electron burst for all r-e- α (^{257}Rf) events was fit using a maximum likelihood method with an exponential decay, yielding a half life of $134.9 \pm 7.7 \mu\text{s}$ for the isomeric state. Qian *et al.* [20] collected 22 r-e- α (^{257}Rf) events, and they measured a half life of $160^{+42}_{-31} \mu\text{s}$, which is in agreement with our value.

The γ -ray spectrum obtained in prompt coincidence with the electron bursts for all r-e events that did not have a spontaneous fission event following the electron is shown in Fig. 2. K-shell X-rays at energies expected for Rf [21] are seen (marked with an asterisk), along with a few prominent γ lines which are attributed to ^{257}Rf . While the γ -ray statistics are low, the presence of two high-energy γ lines at 446 keV and 585 keV may be attributed to the decay of the isomer. This work represents the first observation of any significant γ rays originating from the isomeric decay of ^{257}Rf . Qian *et al.* [20] observed seven γ -ray events in coincidence with a delayed electron event, but could only identify two counts associated with K-shell X-rays.

Our data supports the findings of Qian *et al.* [20] and adds further information to the level scheme of ^{257}Rf . The differences in rotational energy levels built on the $[725]11/2^-$ state were calculated using the simple rotational model. Possible γ lines matching these rotational energy differences were found within the γ -ray energy spectrum in Fig. 2 and labeled with a red circle. On this basis, we present a postulated decay scenario, which is shown in Fig. 3. Additional support for the decay scenario comes from looking at the total excitation energy for r-e- α (^{257}Rf) events, which is the sum of the electron and γ -ray energies for each event. We observe an energy spectrum that ends at a maximum energy of ≈ 1050 keV. The energy difference between the $[725]11/2^-$ state and the $134 \mu\text{s}$ isomeric state is 1080 keV based on our proposed decay scenario, which is comparable to the observed excitation energy.

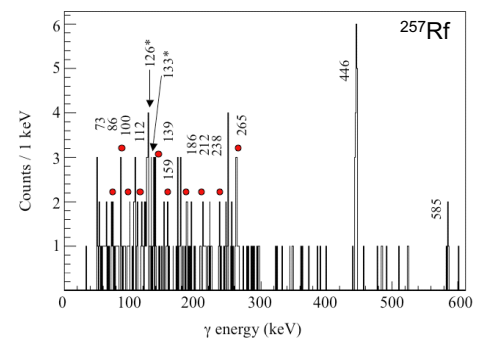


Figure 2: Energy spectrum of gamma rays in coincidence with electron bursts from ^{257}Rf for all r-e events that did not have a spontaneous fission event following the electron. Asterisks indicate known Rf X-rays. The red circles represent gamma-ray lines that match the transition energies calculated with the rotational model.

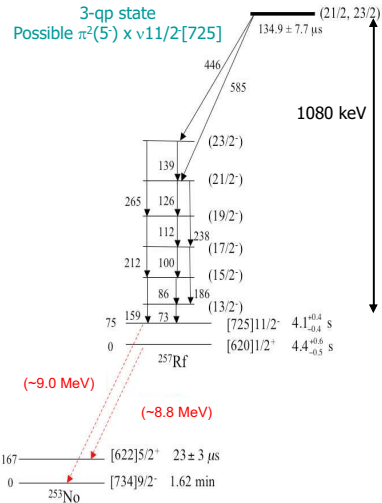


Figure 3: Proposed decay scenario for ^{257}Rf . The figure is based on data from the present work and from Qian *et al.* [20].

Further support for the proposed decay scenario is obtained from examining the hindrance factors of transitions depopulating the isomer. F_W was determined for the $134 \mu\text{s}$ state assuming the 446 keV γ line has a 100% branching ratio, B_γ , and calculated for $E1$, $M1$, and $E2$ transitions. When compared to the estimates by Löbner [22], the possible transitions yield a ΔK value of 4, 5 or 6. The calculations in Ref. [20], using a Woods-Saxon potential [23] and the Lipkin-Nogami [24] prescription for pairing, yield a number of possible 3-qp states. These include $[\pi^2\{[624]9/2^+ \otimes [521]1/2^-\}_{K=5^-} \otimes \nu[725]11/2^-]_{K=21/2}$ or $[\pi^2\{[514]7/2^- \otimes [512]5/2^-\}_{K=6^+} \otimes \nu[725]11/2^-]_{K=23/2}$, at excitation energies of $\approx 1125 \text{ keV}$ and $\approx 1400 \text{ keV}$, respectively. A transition from the $K = 21/2$ state or the $K = 23/2$ state to states built on the $[725]11/2^-$ rotational band would yield a ΔK value of 5 or 6, respectively. It appears that the $134 \mu\text{s}$ isomeric state could be based on one of these 3-qp configurations [19].

3.3. Decay of ^{261}Sg

The results discussed below on ^{261}Sg were first reported by our group in the paper by Berryman *et al.* [19]. ^{261}Sg recoils were identified by observing a characteristic ^{261}Sg α decay ($9.2 \text{ MeV} < E_\alpha < 10.0 \text{ MeV}$) anti-coincident with the MWPC [denoted as $r-\alpha(^{261}\text{Sg})$ events] or observing an “escape” ^{261}Sg α decay followed by the α decay of the daughter nucleus ^{257}Rf ($8.4 \text{ MeV} < E_\alpha < 9.2 \text{ MeV}$) [denoted as $r-x(^{261}\text{Sg})-\alpha(^{257}\text{Rf})$] in the same pixel of the DSSD, following Sg implantation. An escape ^{261}Sg α decay is defined as a detected α that leaves the face of the DSSD, thus depositing only partial energy ($0.5 \text{ MeV} < E_{\text{escape}} < 7.5 \text{ MeV}$). The half life of $r-\alpha(^{261}\text{Sg})$ events was measured to be $178 \pm 14 \text{ ms}$, which agrees with the value of $184 \pm 5 \text{ ms}$ measured by Štreicher *et al.* [26]. Our analysis of the α decay energies agrees with prior measurements [14, 26], and does not add any additional information to the previous α decay studies.

A total of 24 $r-e-\alpha(^{261}\text{Sg})$ events and 15 $r-e-x(^{261}\text{Sg})-\alpha(^{257}\text{Rf})$ events were identified. The energy distribution of the electron bursts for $r-e-\alpha(^{261}\text{Sg})$ or $r-e-x(^{261}\text{Sg})-\alpha(^{257}\text{Rf})$ events is shown in Fig. 4, indicating a maximum energy of $\approx 200 \text{ keV}$. The time difference between recoil implants and the subsequent electron burst is shown in the inset of Fig. 4.

Figure 4: Electron energy spectrum from $r-e-\alpha(^{261}\text{Sg})$ or $r-e-x(^{261}\text{Sg})-\alpha(^{257}\text{Rf})$ events with an inset showing the electron decay curve. The solid line represents the fit to the decay curve, performed with a maximum likelihood method with an exponential decay. The upper and lower dashed lines are described in the text.

The fit was constructed using a maximum likelihood method with an exponential decay, yielding a half life of $9.0^{+2.0}_{-1.5} \mu\text{s}$ for the isomeric state. Upper and lower limits were calculated which encompass 68% of the probability in a Poisson distribution centered on the number of counts expected during the interval from the most probable fit, following the method by Gregorich [27]. It should be noted that there is the possibility of the isomer decaying during the $\approx 15 \mu\text{s}$ deadtime of the data acquisition, and thus only those events occurring $15 \mu\text{s}$ after implantation

were included in Fig. 4.

Previous α -decay data has shown ^{261}Sg to have a ground state spin and parity of $3/2^+$, which has been assigned to the [622]3/2 $^+$ Nilsson orbital [14, 26]. Macroscopic-microscopic calculations [28] place neutron orbitals [725]11/2 $^-$, [613]7/2 $^+$, and [734]9/2 $^+$ within 300 keV of the ground state. In this work, a 9.0 μs isomeric state, which is likely a 1-qp state, was observed with an excitation energy of \approx 200 keV. Although no γ rays were observed directly, any γ ray emitted from the isomeric state must have an energy of less than the total excitation energy of 200 keV. The hindrance factor F_w was determined for the 9.0 μs isomeric state for the three most probable multipole transitions at a few different energies to estimate the ΔK . The likely transition can then be determined based on these calculated hindrance factors and estimates by Löbner [22]. We conclude that the most likely scenario is that the isomer must originate from the [725]11/2 $^-$ state and decay to the rotational band built on the [613]7/2 $^+$ Nilsson state via a $\Delta K = 2$, $E1$ transition [19]. This work represents the first observation of the electromagnetic decay of an excited state in any nucleus with $Z > 104$.

Acknowledgments

The authors thank the 88-Inch Cyclotron operations staff for providing the beams for this experiment. The work was supported in part by the U.S. DOE under Contract No. DE-AC02-05CH11231 (LBNL) and under Grant Nos. DE-FG52-06NA26206 and DE-FG02-05ER41379. Part of this work was performed under the auspices of the US Department of Energy Lawrence Livermore National Laboratory under Contract No. DE-AC52-07NA27344.

References

- [1] S. Ćwiok, J. Dobaczewski, P.-H. Heenen, P. Magierski, and W. Nazarewicz, Nucl. Phys. A **611**, 211 (1996).
- [2] A.V. Afanasjev, T.L. Khoo, S. Frauendorf, G.A. Lalazissis, and I. Ahmad, Phys. Rev. C **67**, 024309 (2003).
- [3] M. Bender, K. Rutz, P.-G. Reinhard, J. A. Maruhn, and W. Greiner, Phys. Rev. C **60**, 034304 (1999).
- [4] Yu. Ts. Oganessian *et al.*, Phys. Rev. Lett. **83**, 3154 (1999).
- [5] L. Stavsetra *et al.*, Phys. Rev. Lett. **103**, 132502 (2009).
- [6] Yu. Ts. Oganessian *et al.*, Phys. Rev. C **74**, 044602 (2006).
- [7] Yu. Ts. Oganessian *et al.*, Phys. Rev. C **69**, 054607 (2004).
- [8] M. Leino and F.P. Hessberger, Annu. Rev. Nucl. Part. Sci. **54**, 175 (2004); R.D. Herzberg and P.T. Greenles, Prog. Part. Nucl. Physics **61**, 674 (2008).
- [9] C.M. Folden III, Ph.D. thesis, University of California, Berkeley, Report No. LBNL-56749 (2004).
- [10] G. Duchêne *et al.*, Nucl. Instrum. Methods A **432**, 90 (1999).
- [11] G.D. Jones, Nucl. Instrum. Methods A **488**, 471 (2002).
- [12] A.V. Belozerov *et al.*, Eur. Phys. J. A **16**, 447 (2003).
- [13] I. Dragojević *et al.*, Phys. Rev. C **78**, 024605 (2008).
- [14] S. Antalic *et al.*, Acta. Physica Slovaca **56**, 87 (2006).
- [15] R.M. Clark *et al.*, Phys. Lett. B **690**, 19 (2010).
- [16] R.-D. Herzberg *et al.*, Nature **442**, 896 (2006).
- [17] S.K. Tandel *et al.*, Phys. Rev. Lett. **97**, 082502 (2006).
- [18] F.P. Heßberger *et al.*, Eur. Phys. J. A **43**, 55 (2010).
- [19] J.S. Berryman *et al.*, Phys. Rev. C **81**, 064325 (2010).
- [20] J. Qian *et al.*, Phys. Rev. C **79**, 064319 (2009).
- [21] *Table of Isotopes*, 8th ed., edited by R. Firestone and V. Shirley (Wiley, New York, 1996).
- [22] K.E.G. Löbner, Phys. Lett. **26B**, 369 (1968).
- [23] S. Ćwiok, J. Dudek, W. Nazarewicz, J. Skalski, and T. Werner, Comput. Phys. Commun. **46**, 379 (1987).
- [24] Y. Nogami, Phys. Rev. **134**, B313 (1964).
- [25] F.P. Heßberger, Phys. At. Nucl. **70**, 1445 (2007).
- [26] B. Štreicher *et al.*, Acta Phys. Pol. **38**, 1561 (2007).
- [27] K.E. Gregorich, Nucl. Instrum. Methods A **302**, 135 (1991).
- [28] A. Parkhomenko and A. Sobiczewski, Acta. Physica Polonica B **36**, 3115 (2005).